Design and experimental validation of an optimal remixing procedure for vanadium flow batteries affected by faradaic imbalance

Thomas Puleston[a,b,*], Andrea Trovò[b,c], Giacomo Marini[b,c], Maria Serra[a], Ramon Costa-Castelló[a], Massimo Guarnieri[b,c]

[a]*Institut de Robòtica i Informàtica Industrial, CSIC-UPC, C/ Llorens i Artigas 4-6, 08028, Barcelona, Spain*
[b]*Department of Industrial Engineering, University of Padua, Via Gradenigo 6a, 35131, Padova, Italy*
[c]*Interdepartmental Centre Giorgio Levi Cases for Energy Economics and Technology, University of Padua, Via Gradenigo 6a, 35131, Padova, Italy*

Abstract

A novel optimised partial remixing procedure for recovering the capacity loss in vanadium flow batteries that suffer from electrolyte imbalance is implemented and its practical performance is thoroughly evaluated in this paper. The proposed optimal remixing method is assessed by means of experimental tests and compared to the conventional total remixing and to the hydraulic bypass connection between the electrolyte tanks. Special attention is given to the interaction between stoichiometric imbalance, caused by crossover through the membrane, and faradaic imbalance, caused by side reactions that produce a shift in the average oxidation state of the electrolyte. Consistently with the theoretical predictions, it is shown that in actual flow batteries operation, the effectiveness of the conventional remixing methods is very limited when oxidation constitutes the main source of imbalance. In contrast, the proposed optimal remixing allows a substantial capacity recovery, mitigating up to a 67% of the capacity loss originated by oxidation without requiring any additional equipment.

Keywords: Vanadium flow battery, State of Health, side reactions, capacity loss, electrolyte imbalance

*Corresponding Author
Email address: tpuleston@iri.upc.edu (Thomas Puleston)

1. Introduction

Renewable energy sources (RES) are recognised as the only viable solution to mitigate climate changes and fossil fuels depletion, so that substantial efforts are being made by governments, international organisations and companies to support their implementation towards a sustainable energy system. As an illustration of these increasingly ambitious goals, the European Union has recently revised its RES target for 2030, elevating their penetration from 32.8% to 40.5% [1]. Energy storage systems (ESSs) play a crucial role in the RES integration into the grid, providing the means to cope with the intermittent, unpredictable and thus non-dispatchable nature of RESs [2, 3].

Among the different ESSs developed so far, flow batteries are considered one of the most promising technologies for large-scale stationary applications [4]. In conventional closed batteries, the electrodes have the double function of hosting the electrochemical reaction and storing the reactants active species. In contrast, flow batteries use fluid electrolytes which are stored in tanks separated from the electrochemical reactor where power conversion occurs, resulting in a decoupling of energy and power [5]. The high degree of versatility and scalability associated with this particular architecture is combined with a respectable efficiency (75–85%), low maintenance requirements, and a minimal self discharge rate when off-service. The All-Vanadium Flow Battery (VFB) is the most mature flow battery technology, with important industrial-scale facilities already in service worldwide [6]. They use two ions of vanadium in the negolyte (negative electrolyte), V^{2+} and V^{3+}, and two ions in the posolyte (positive electrolyte), VO^{2+} and VO_2^+, respectively abbreviated as V^{II}, V^{III}, V^{IV}, and V^{V}, because of the oxidation state of vanadium in these ions. By utilising only vanadium as the active element, they do not suffer from the cross contamination problems that affect other types of flow batteries, allowing a very long service life (ca. 20,000 cycles are claimed by manufacturers). In addition, they do not pose significant safety concerns because of the utilisation of aqueous electrolytes at room temperature and atmospheric pressure.

Despite these remarkable advantages, the FB particular structure poses some important challenges, mostly related to undesired side effects. One of them rises from the discrepancy of reactant concentrations at the positive and negative side of the system [7, 8]. This condition, known as elec-

trolyte imbalance, constitutes the main cause of capacity loss in VFBs, and may lead to even more severe consequences such as electrode corrosion or membrane damage [9, 10]. Electrolyte imbalance can be classified in "Stoichiometric Imbalance"(or "Mass Imbalance") and "Faradaic Imbalance" (or "Oxidative/Reductive Imbalance") [11, 12]. The former is a consequence of vanadium crossover through the cell membranes that results in a different amount of vanadium moles on each side of the system [13]. The latter is caused by some side reactions which involve electron transfer with species other than vanadium ions, resulting in a deviation from the ideal overall Average Oxidation State (AOS) of +3.5. When faradaic imbalance leads to an AOS higher than +3.5 it can also be denominated "Oxidative Imbalance", and is typically originated by hydrogen evolution reaction at the negative electrode during charge, or air oxidation of V^{II} at the negative tank when this is not perfectly sealed. A shift towards an AOS lower than +3.5 is known as "Reductive Imbalance", which is far less common than oxidative imbalance and can be caused by precipitation of V^{V} at high temperatures, corrosion of solid components with simultaneous reduction of V^{V}, as well as oxygen evolution reaction at the positive electrode [14].

Several methods have been developed to offset VFB imbalance. It was demonstrated that the most suitable recovery strategy is strongly dependent on the type of imbalance that is affecting the battery. In particular, stoichiometric imbalance can be reset in a relatively simple manner by remixing the tanks contents and equally distributing the resulting solution, thus equalising the volumes and concentrations in both tanks at the oxidation state $V^{3.5+}$ [15, 16]. Although this method is simple and effective, it causes the VFB to fall in an under-discharged condition, involving an out-of-service for some time and the loss of the stored energy. Conversely, if the concentrations and volumes in each tank are perfectly known, a partial remixing consisting of transferring just the proper amount of electrolyte to equalise the number of moles in both tanks can be conducted to avoid the shortcomings of the total remixing [17, 9]. Another way to limit the extent of volume imbalance, and thus stoichimetric imbalance, is to utilise an anti-syphoning pipe to allow solution to transfer from one side to the other if the electrolytes exceed preset levels, as described in [18]. Alternatively, a thin valved pipe connecting the two tanks at their bottom can be used to keep the tanks levelled, hence minimising this type of imbalance [19]. Other authors have proposed different methods to slow down the progression of the imbalance. For instance, Lu et al. [20] showed that crossover can be mitigated by setting either an

asymmetric vanadium concentration or asymmetric operating pressures to induce a convective flux through the membranes in an opposite direction to the natural diffusive flux. More recently, Shin et al. [21] and Toja et al. [22] demonstrated that vanadium crossover and volume change can also be mitigated by increasing sulphuric acid concentration at the negative electrolyte. However, this approach requires careful trimming, as an excessive increase in the sulphuric acid concentration may reduce the solubility of V^{II} and V^{III}, possibly leading to the precipitation of these ions [23].

The faradaic imbalance is much more complex to address, because the shift in the AOS cannot be restored by remixing the electrolytes, i.e., the resulting solution will not be a mixture of V^{III} and V^{IV} in proportion 1:1 as in the stoichiometric imbalance, so that the capacity of the VFB will remain diminished after remixing [17, 24]. Consequently, more sophisticated chemical or electrochemical methods are required to regenerate the original AOS of +3.5. Skyllas-Kazacos and co-workers [25] developed a procedure, later systematised by Roznyatovskaya et al. [26], which allows to fully correct faradaic imbalance by charging the imbalanced electrolytes, and subsequently replacing a part of the posolyte by a V^{IV} solution or fresh $V^{3.5+}$ electrolyte. In spite of being simple and effective, such method requires of an externally supplied electrolyte to compensate the removed quantity, somewhat limiting its applicability. In [27], an alternative hydraulic circuit connecting the tanks to each other is provided which is activated when the VFB is operated in "recovery mode", resulting in the full mixing of the electrolytes. Afterwards, the desired AOS of +3.5 is restored by means of an electrolysis cell. This cell utilises an auxiliary electrolyte to reduce the vanadium and an optical sensor detects the proper endpoint of the process. More recently, Poli et al. [14] and Piguchov et al. [28] proposed to couple the system with an electrochemical cell that is placed in parallel to the main hydraulic circuit. These methods offer the advantages of not interrupting the VFB operation and of not requiring an auxiliary reducting agent. Instead, the oxidation reaction that provides the electrons for the reduction of V^{V} contained in the positive electrolyte is the oxygen evolution reaction, which is induced by titanium-based electrodes at the electrolysis cell. Finally, it was also proposed to regenerate the electrolyte by adding a reducing/oxidising chemical agent to the system, such as oxalic acid [29], ethanol or methanol [30, 31].

It is important to mention that the side effects causing both faradaic and stoichiometric imbalances may occur even when the battery is correctly operated, leading to major imbalance and capacity reduction after prolonged

operation. In this framework, new methods capable of dealing with both types of imbalance simultaneously can become crucial, especially for those facilities which lack of chemical/electrochemical equipment for the complete correction of faradaic imbalance. In a previous work [32], some of these authors analysed the effects of electrolyte imbalance on the battery capacity and deduced that stoichiometric and faradaic imbalances interact with each other. Based on those findings, this work implements and experimentally validates a cost-effective optimal remixing procedure that allows to recover up to a 67% of the capacity loss originated by faradaic imbalance. This method allows to reduce the frequency of scheduled chemical/electrochemical maintenance for 100% recovery of faradaic imbalance in commercial VFBs and eliminates the battery out-of-service in the event of unforeseen issues, such as an accelerated oxidation due to imperfect tank sealing. To complete the experimental study, the proposal is experimentally contrasted with other typical approaches for minimising imbalance effects, i.e., the standard total remixing and the bypass connection for keeping the tanks volumes levelled. To the best of our knowledge, this is the first experimentally validated capacity recovery method that considers the combined effect of both types of imbalances. Furthermore, it is the only method that allows to mitigate the capacity loss associated to faradaic imbalance without resorting to any additional equipment or treatment apart from those required in a standard remixing procedure.

The paper is organised as follows. Section 2 introduces the theoretical framework upon which the presented capacity recovery method stands. Section 3 presents the design and implementation of the optimal remixing method together with the experimental setup utilised for its validation. Section 4 presents the results and discussion of the experimental study. Finally, Section 5 collects the main conclusions drawn from the investigations.

2. Theoretical background

Vanadium flow batteries consist of two tanks that store aqueous solutions of different vanadium redox couples in sulphuric acid (see Figure 1a). When the battery is operating, the electrolytes are pumped from the tanks to the electrochemical cells (or stack of cells), which convert the chemical energy of the electrolytes into electric power or vice versa. The cell electrodes, where the posolyte and the negolyte circulate, are separated by a selective ion-exchange membrane that allows ions to flow but not electrons, thus clos-

ing the electric circuit. The electrolytes flowing out of the cells are poured back in the electrolyte tanks, thus closing the hydraulic system. The main electrochemical reactions that take place in the cells are:

$$\text{Negative electrode:} \qquad \mathrm{V^{2+}} \underset{charge}{\overset{discharge}{\rightleftharpoons}} \mathrm{V^{3+}} + e^- \tag{1}$$

$$\text{Positive electrode:} \qquad \mathrm{VO_2^+} + 2\mathrm{H^+} + e^- \underset{charge}{\overset{discharge}{\rightleftharpoons}} \mathrm{VO^{2+}} + \mathrm{H_2O} \tag{2}$$

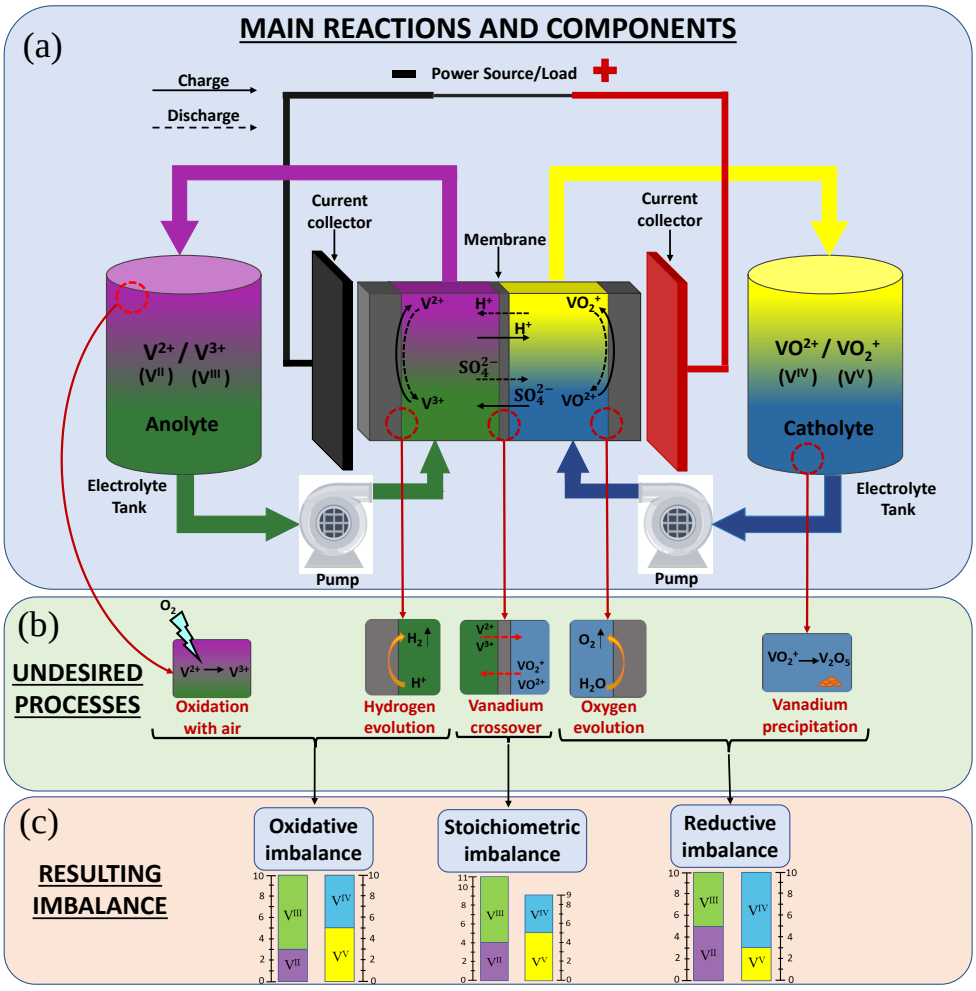

Figure 1: Single-cell scheme of a VFB: a) main components and electrochemical reactions; b) main undesired processes; and c) resulting imbalances.

Vanadium flow batteries are expected to be balanced, meaning that the number of moles of V^{II} and V^{III} at the negolyte are equal to the number of moles of V^{V} and V^{IV} at the posolyte, respectively. In general, though not necessarily, this condition implies that both tanks contain the same volume of liquid, and the concentrations of V^{II} and V^{III} at the negolyte are equal to the concentrations of V^{V} and V^{IV} at the posolyte. Ideally, if the electrolytes are originally balanced, and (1) and (2) are the only reactions occurring in the system, and no vanadium crossover occurs, the VFB remains balanced. When the flow battery is balanced, all moles of active species are available to participate in the electrochemical conversion reactions, so that its capacity is maximum. Conversely, the battery capacity decreases as the electrolytes deviate from that condition [9].

However, as a result of crossover and the side reactions described in Section 1, VFBs normally become imbalanced after prolonged operation (see Figure 1b and 1c). By looking at these figures, it is easy to visualise how an asymmetric crossover results in a different number of moles contained in each side of the system, namely, in stoichiometric imbalance, while the side reactions result in a net oxidation or reduction of the vanadium species, i.e., in faradaic imbalance. In the case of faradaic imbalance caused by hydrogen evolution, a fraction of the electrons released by the oxidation of V^{IV} are captured by the protons instead of vanadium ions, not producing the reduction of V^{III} to V^{II}. Analogously, a similar process occurs with the oxygen evolution at the positive electrode.

The imbalance results in a decline of the State of Health (SoH), which compares the actual capacity of the battery (Q_M) with the total capacity corresponding to a balanced condition (Q_M^N):

$$\mathrm{SoH} = \frac{Q_M}{Q_M^N}. \tag{3}$$

In a previous work [32], a generalised expression was derived to calculate the SoH of a VFB under any level of faradaic and stoichiometric imbalance in terms of the number of vanadium moles in the system:

$$\mathrm{SoH} = \frac{\min\{M_2, M_5\} + \min\{M_3, M_4\}}{M_t/2}, \tag{4}$$

where M_i is the number of moles of vanadium ions with oxidation state $+i$, and M_t is the total number of vanadium moles in the system: $M_t =$

$M_2 + M_3 + M_4 + M_5$. The numerator of (4) represents the total number of moles that are able to participate in the electrochemical reactions with the actual imbalance condition. It is given by the number of moles that are currently available for participating in the discharge reaction ($\min\{M_2, M_5\}$) plus the number of moles that are available for participating in the charge reaction ($\min\{M_3, M_4\}$), resulting in the number of moles which react from fully charged to fully discharged. In turn, the denominator ($M_t/2$) represents the total number of moles that would participate in the reaction from fully charged to fully discharged if the VFB were perfectly balanced. An illustrative example of equation (4) is presented in Figure 2a, which shows that, as a result of imbalance, only 7 moles of vanadium ions are able to react when the battery goes from fully charged to fully discharged, in comparison to the 10 moles that would be able to react in a balanced condition. Note that, in the "fully charged" state there is still V^{III} present in the negolyte, whereas in the "fully discharged" state there is V^{V} in the posolyte, because, due to the lack of counterpart ions, these species are not able to participate in the further charging/discharging reactions, which results in a capacity loss.

(a)

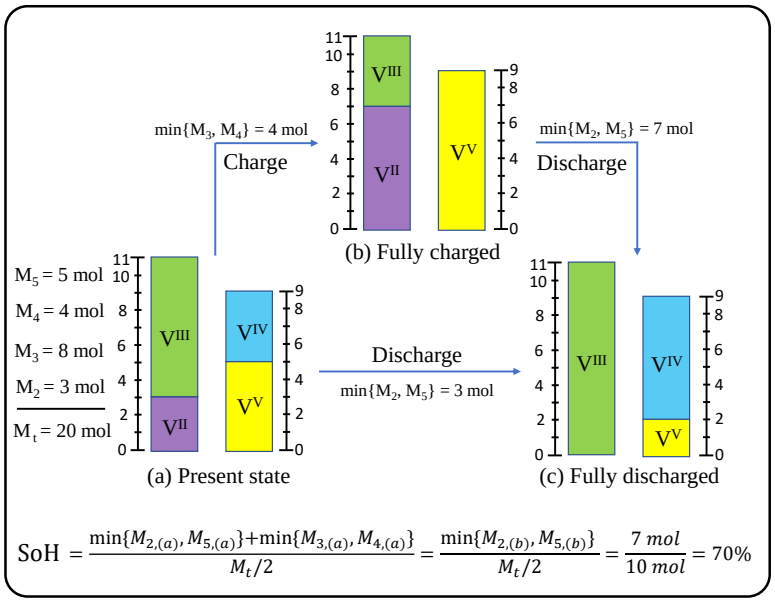

(b)

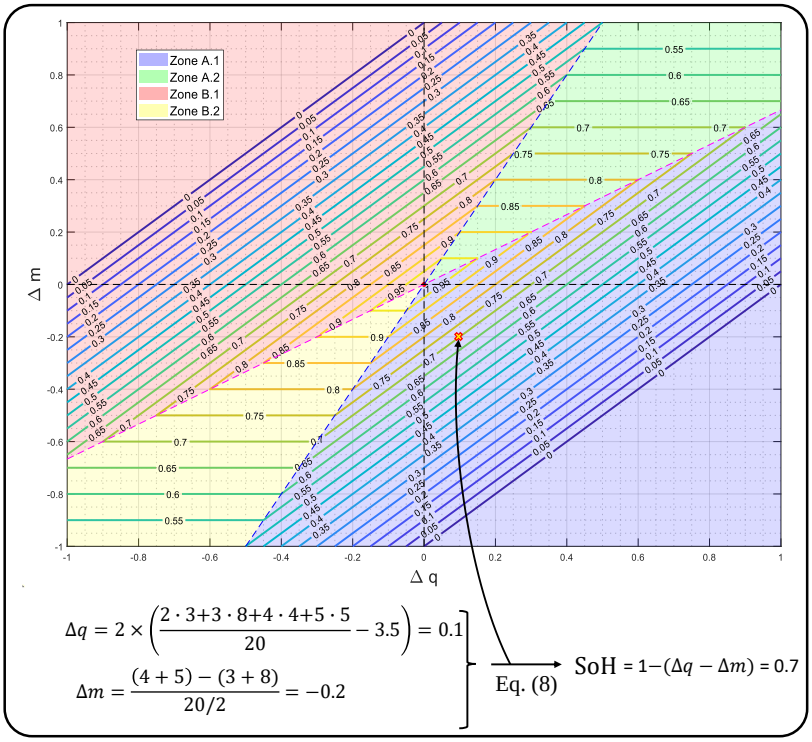

Figure 2: (a) Graphical demonstration of generalised SoH equation (4). (b) SoH contour curves of (8) and (9) on the Δq-Δm imbalance map, with represented example of imbalance sketched in Fig. 2a.

Eq. (4) does not allow to visualise the individual effects of faradaic and stoichiometric imbalance, let alone appreciating their interaction. In order to clearly separate the two sources of imbalance, we define a "Stoichiometric Imbalance Index" Δm, and a "Faradaic Imbalance Index" Δq. Since the stoichiometric imbalance is related to an asymmetric number of vanadium moles in the two tanks, Δm can be expressed as the difference between the total number of vanadium moles in the posolyte and the negolyte, normalised to the ideal number of moles in each tank in a balanced condition:

$$\Delta m = \frac{(M_4 + M_5) - (M_2 + M_3)}{M_t/2}. \tag{5}$$

In turn, the faradaic imbalance is related to a shift in the AOS from its ideal value of +3.5 [11]:

$$\text{AOS} = 2\frac{M_2}{M_t} + 3\frac{M_3}{M_t} + 4\frac{M_4}{M_t} + 5\frac{M_5}{M_t}, \tag{6}$$

so that its index can be defined as:

$$\Delta q = 2(\text{AOS} - 3.5) \tag{7}$$

Based on the definitions of Δq and Δm, we rewrite (4) into a more convenient form, that explicitly decouples the effects of stoichiometric and faradaic imbalances (see proof in [32]). The resulting expression is a piecewise function that present different forms in four different domains (later "Zones").

Zone A pertains to the condition $\Delta m \leq 2\Delta q$, where the SoH assumes the expression:

$$\text{SoH} = 1\text{–max}\{\Delta q\text{–}\Delta m\ ,\ \Delta m/2\} \tag{8}$$

Zone B pertains to the condition $\Delta m > 2\Delta q$, where the SoH assumes the expression:

$$\text{SoH} = 1\text{–max}\{\Delta m\text{–}\Delta q\ ,\ -\Delta m/2\} \tag{9}$$

Zones A and B can be each separated in two sub-domains, as expressed in Table 1. Note that the indexes Δm and Δq may be either positive or negative.

Table 1: Expression for the SoH in terms of Δm and Δq.

Zone	**Primary condition**	**Secondary condition**	**SoH expression**
A.1	$\Delta m \leq 2\Delta q$	$\Delta m \leq \frac{2}{3}\Delta q$	$1-(\Delta q - \Delta m)$
A.2	$\Delta m \leq 2\Delta q$	$\Delta m > \frac{2}{3}\Delta q$	$1-\frac{1}{2}\Delta m$
B.1	$\Delta m > 2\Delta q$	$\Delta m \geq \frac{2}{3}\Delta q$	$1-(\Delta m - \Delta q)$
B.2	$\Delta m > 2\Delta q$	$\Delta m < \frac{2}{3}\Delta q$	$1+\frac{1}{2}\Delta m$

Figure 2b shows the SoH contour curves, namely, capacity isolines, obtained from (8) and (9), as functions of Δq and Δm. Besides, the condition of the electrolyte presented in the previous example (Figure 2a) is indicated in the plane. Note that, consistently with the direct analysis made with (4), it results that the SoH = 70%. Moreover, it is now possible to quantify the level of faradaic and stoichiometric imbalance of the system and, more importantly, to see how possible changes in the imbalance condition would influence the battery SoH.

The main outcome of equations (8) and (9) is that, for any level of faradaic imbalance, there will be an optimal stoichiometric imbalance that maximises the battery capacity. Specifically, this maximum is located at the line $\Delta m = 2/3\ \Delta q$, namely, at the border between zones A.1 and A.2, and zones B.1 and B.2. This result can be appreciated in Figure 2b and is formally proved in [32]. Equations (8) and (9) yield $\text{SoH}(\Delta m = 0) = 1 - |\Delta q|$, while $\text{SoH}(\Delta m = 2/3\Delta q) = 1 - 1/3|\Delta q|$. Therefore, it is concluded that the condition $\Delta m = 0$ maximises the capacity only if Δq=0, whereas in the case of faradaic imbalance, $\Delta q \neq 0$, the capacity loss with $\Delta m = 2/3\Delta q$ is one third of that with $\Delta m = 0$, i.e., with perfectly balanced electrolyte masses. Since the stoichiometric imbalance can be modified in a much simpler way than the faradaic one by a simple redistribution of the tanks contents, this result is used as the basis for the optimal partial remixing method that is presented in the next section.

3. Optimal remixing design and implementation

This section presents the methodology for the implementation of the optimised partial remixing procedure (later "optimal remixing"), together with the specific setup utilised for its validation. The experimental test bench is

described in Section 3.1, the experimental protocols are outlined in Section 3.2, and the steps of the optimal remixing procedure in terms of the available information are presented in Section 3.3.

3.1. Experimental setup

The experimental tests were run on the CTF (Cell Test Facility) test bench shown in Fig. 3a and 3b, which is in operation at the Electrochemical Energy Storage and Conversion Laboratory (EESCoLab) of the University of Padua. The main cell consisted of a single-cell (Pinflow, Czechia) with an active area of 50 cm^2 equipped with SGL GFD 4.65 EA thermally treated graphite felt electrodes (Sigracell, Germany) in a flow-through configuration, and a FAPQ330 anion exchange membrane separator (Fumatech GmbH, Germany). An Open Circuit Voltage (OCV) cell (Pinflow, Czechia) equipped with a leakless Ag/AgCl reference electrode (Pinflow, Czechia) provided half-cell voltage monitoring. The two cells were connected hydraulically in series, with the OCV cell at the inlets on the main cell, as shown in Figure 3a.

The electrolyte tanks had a capacity of 600 ml each and were equipped with magnetic stirrers (Anzeser, China) to ensure uniform species concentrations. The electrolyte (GfE GmbH, Germany) had an AOS of +3.5 and total vanadium concentration of 1.6 $mol \cdot l^{-1}$, with 2 $mol \cdot l^{-1}$ of sulphuric acid and 0.05 $mol \cdot l^{-1}$ of phosphoric acid. The tanks were interconnected with a valved bypass pipe that allowed to keep the same volume of electrolyte in both tanks. The negative electrolyte tank was connected to a nitrogen line that allowed to exclude the presence of atmospheric oxygen in the residual volume, thus preventing V^{2+} oxidation. The nitrogen had been humidified to avoid evaporation of water from the electrolyte, and its flow rate was set by means of a manual valve.

A two-channel peristaltic pump (LeadFluid BT600L, China) controlled the flow rate. The power conditioning system (PCS) consisted of a charging power supply (Rigol, China) and a discharging electronic load (Chroma, Taiwan), which allowed to modulate the current/voltage profiles in galvanostatic/potentiostatic modes. The instrumentation included differential pressure sensors at the inlet and outlet of the main cell and temperature sensors in each electrolyte tank. The entire setup was installed in a thermal chamber (Binder, Germany), to keep tightly constant the system temperature.

The CTF operation was controlled and monitored by a Battery Management System (BMS) made of a desktop computer and Compact DAQ data

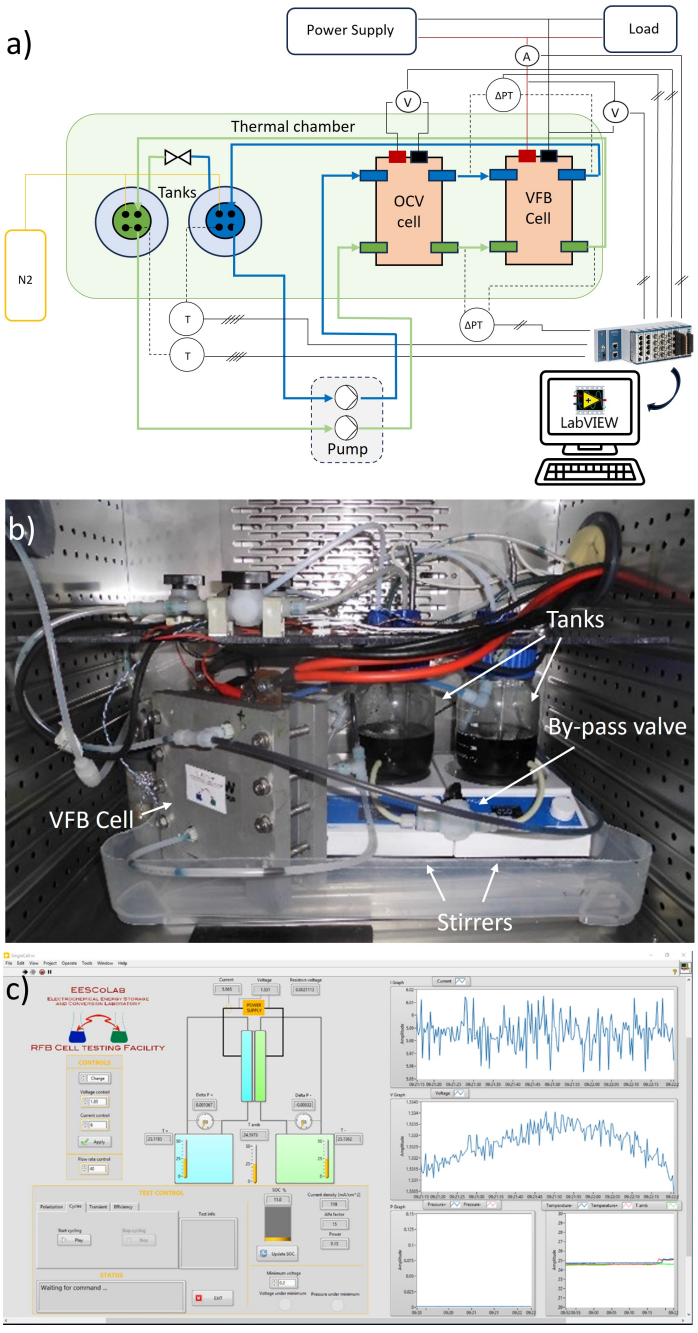

Figure 3: a) Schematic diagram of the experimental setup, where T stands for temperature sensor, ΔPT for differential pressure transmitter, A for current sensor, and V for voltage acquisition channel. b) Detail of the components inserted in the thermal chamber. c) User interface of the control software.

acquisition system (National Instruments, US) hardware running in-house LabVIEW software (Fig. 3c) [33].

3.2. Experiment protocols

This subsection presents the general experimental conditions of the tests that are conducted in Section 4 for validating optimal partial remixing method along with the theory presented in Section 2. In all tests, each tank was initially filled with 290 ml of fresh electrolyte. The system was firstly pre-charged at constant current of 2 A to convert all V^{IV} into V^{III} in the negolyte and all V^{III} into V^{IV} in the posolyte. This pre-charging phase allows to generate to the two vanadium couples of the VFB. After this phase was concluded, the battery underwent a number of charge/discharge cycles, in order to produce a significant electrolyte imbalance, hence, a meaningful capacity loss. The cycles were run at Constant Current / Constant Voltage (CC-CV), which consists in charging (discharging) the battery at constant current until reaching a maximum (minimum) voltage threshold when the operation switches to constant voltage and the current gradually decreases until reaching a minimum cutoff value at which the charging (discharging) is completed. This commutation from CC to CV ensured a high level of utilisation of the available vanadium reactants while preventing dangerous high overpotentials at low reactant concentrations, i.e., at extreme SoC values. In the CC phase, the current was 6 A (120 mA/cm^2) and the cutoff voltage was 1.65 V in charge and 0.6 V in discharge. In the CV phase, the voltage was 1.65 V in charge and 0.6 V in discharge, and the cutoff current was 0.1 A both in charge and discharge. The charge and discharge capacity of each cycle was measured with the Coulomb Counting method, namely, by integrating the current over the complete charge and discharge duration, respectively.

The stirrers were kept active throughout the entire experiments, and the thermal chamber maintained the temperature constant at 25 ^{o}C. The flow rates were set at 50 ml/min in all cycles, being this a high enough value for ensuring high flow factor at the applied current level of 6 A. In order to accelerate the V^{II} oxidation so as to produce a significant faradaic imbalance in a reasonable time-span, the nitrogen purge was turned off (except when explicitly indicated further on).

During the experiments, the SoC of each electrolyte was continuously monitored with the half-cell OCV voltage measurements against the reference

electrode, based on the Nernst equation [34, 35]:

$$\text{Negative el.:} \quad E_n = E_n^\theta + \frac{RT}{F}\ln\left(\frac{1-\text{SoC}_\text{n}}{\text{SoC}_\text{n}}\right), \quad \text{SoC}_\text{n} = \frac{M_2}{M_2+M_3} \tag{10a}$$

$$\text{Positive el.:} \quad E_p = E_p^\theta + \frac{RT}{F}\ln\left(\frac{\text{SoC}_\text{p}}{1-\text{SoC}_\text{p}}\right), \quad \text{SoC}_\text{p} = \frac{M_5}{M_4+M_5} \tag{10b}$$

where E_i is the measured half-cell voltage, R the ideal gas constant, T the temperature, F the Faraday constant, E_i^θ is the formal potential against the reference electrode, and the subindexes n and p stand for the negative and positive side, respectively. Each E_i^θ lumps the standard potential with other terms assumed to be constant, such as the activity coefficients and proton concentrations, and corresponds to the measured half-cell voltage when each SoC = 0.5. From eqs. (10) the SoCs as functions of measured voltage were derived as:

$$\text{Negative el.:} \qquad \text{SoC}_\text{n} = \frac{-\exp\left[\frac{F}{RT}(E_n - E_n^\theta)\right]}{1-\exp\left[\frac{F}{RT}(E_n - E_n^\theta)\right]} \tag{11a}$$

$$\text{Positive el.:} \qquad \text{SoC}_\text{p} = \frac{\exp\left[\frac{F}{RT}(E_p - E_p^\theta)\right]}{1+\exp\left[\frac{F}{RT}(E_p - E_p^\theta)\right]}, \tag{11b}$$

3.3. Optimal remixing procedure

The optimal remixing strategy aims to bring the system to the line $\Delta m = 2/3\ \Delta q$ of Figure 2b, in order to maximise the capacity of the VFB compatibly with its actual faradaic imbalance. As discussed in Section 2, the capacity loss on this line is expected to be only one-third of the capacity loss with perfectly balanced electrolyte masses ($\Delta m = 0$). To perform the procedure, only a simple device for transferring electrolyte from one tank to the other is required, which may be the same as the one used for performing the standard total remixing.

Two variants of the optimal remixing can be used, depending on the available information:

- **One-Step Optimal Remixing**. When concentration measurements or estimates are available, the method can be straightforward according to the flowchart of Figure 4a. That information can be obtained either from direct measurements (e.g. potentiometric titration [36] or amperometric measurements [37]), or indirectly from estimation algorithms

(see, for instance, [38] and [39]). In this case, the volume of electrolyte to be transferred in order to reach the optimal Δm is calculated based on the current concentrations.

- **Two-Step Optimal Remixing**. When concentration values are not available, the optimal remixing can be pursued in an indirect way, following the steps presented in Figure 4b. A total remixing is firstly conducted to equalise volumes and concentrations. Then, Δm can be assumed to be approximately equal to zero, and Δq is obtained from (8) as $\Delta q = 1 - \text{SoH}$. Finally, the optimal stoichiometric imbalance is calculated and, accordingly, the necessary volume of electrolyte is transferred in order to reach that point. This variant of the method presents the advantage of not requiring concentration measurements to determine the value of Δq, at the expense of requiring a total remixing before conducting the optimal one.

In these experiments the standard total remixing was conducted with a twofold purpose. On the one hand, to compare the traditional approach with the optimal remixing presented in this paper. On the other hand, to obtain the value of Δq that was required for performing the two-step optimal remixing procedure, as described above. In particular, the standard total remixing was performed as follows:

- **Standard Total Remixing.** Firstly, all the electrolyte in the negative side of the system is transferred to the positive tank. Secondly, the resulting solution is stirred over 5 min to ensure a uniform composition and is subsequently evenly distributed between the two tanks. Finally, a pre-charging process is run to regenerate the vanadium couples of the VFB. To prevent the progression of imbalance during this operation, the nitrogen purge is activated during remixing and pre-charging.

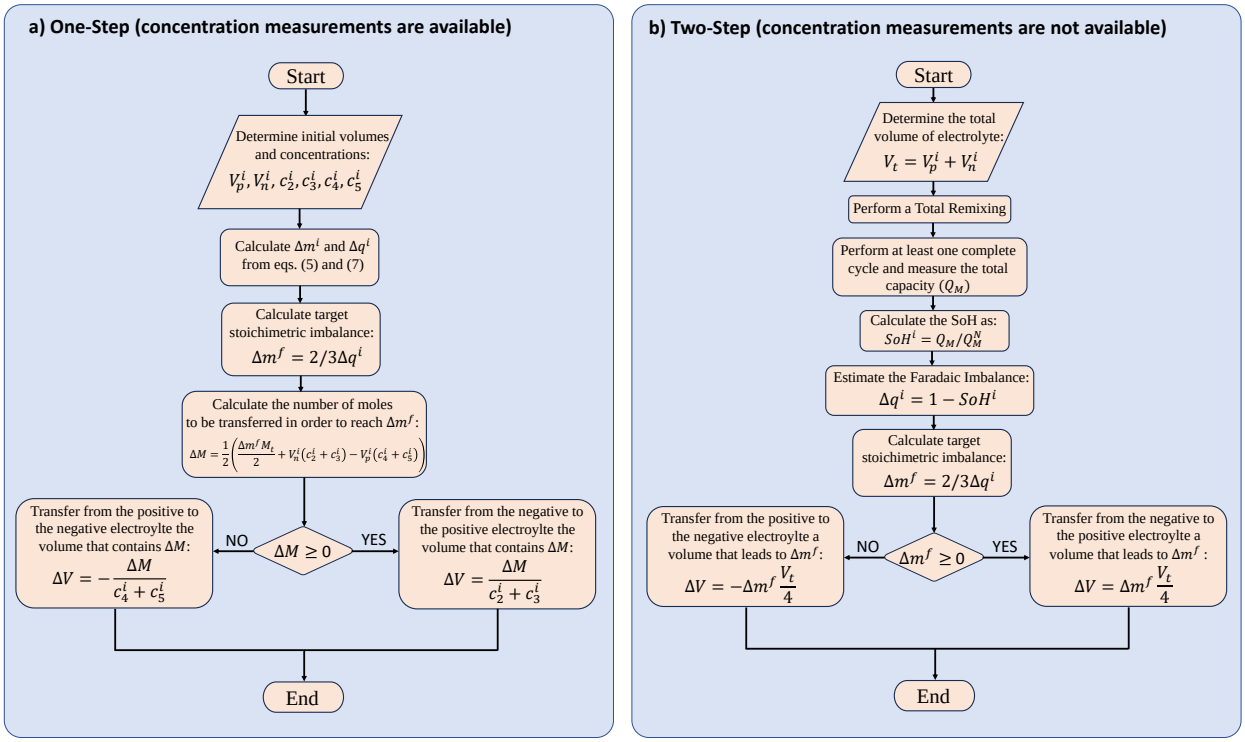

Figure 4: Flowchart of the optimal remixing procedure: a) when concentration measurements are available; b) when concentration measurements are not available. Superscripts i and f indicate the initial condition (before optimal remixing) and the final condition (after optimal remixing), respectively.

4. Experimental results and discussion

In this section, experimental tests are presented to compare and analyse the effectiveness of different experimental methods in minimising the capacity loss of a VFB that suffers from simultaneous faradaic and stoichiometric imbalance. In particular, the optimal remixing method, based on the theoretical findings presented in Section 2 and formulated in Section 3, is tested and compared to the standard total remixing and the hydraulic bypass methods.

4.1. Test 1: Optimal Remixing vs. Total Remixing

This section compares the effects of the total remixing and optimal remixing in facing the capacity loss of a VFB system after its electrolyte imbalance had freely developed. In particular, the two-step variant of the optimal

remixing described in Section 3.3 was implemented, because no concentration measurement was available. The bypass valve between the two tanks was kept close throughout the complete test, hence allowing possible volumetric imbalances. The system are initially in a balanced condition, with 290 ml of fresh $V^{3.5+}$ electrolyte in each tank. After a pre-charging process, the battery underwent 50 charge-discharge CC-CV cycles, as described in Section 3.2. Once these 50 cycles were completed, a total remixing was performed, and two additional cycles were run, in order to assess the total remixing effectiveness in recovering the battery capacity. Finally, based on the capacity achieved with the total remixing, the extent of faradaic imbalance was determined and an optimal remixing followed by two final cycles was performed.

Note that, as a result of self-discharge events, the charge capacity was slightly higher than the discharge capacity. Although this difference is not explicitly considered in the previous sections, the theory presented in Section 2 and the optimal remixing procedure formulated in Section 3.3 can be straightforwardly used provided that the same value Q_M is adopted consistently for all the calculations. In our calculations and analyses the discharge capacity was used for Q_M, but the average between the charge and discharge capacities could have been used alternatively, without affecting the results.

Figure 5a displays the evolution of the battery charge and discharge capacity throughout the complete test. As a consequence of the imbalance, the capacity progressively reduced along the first 50 cycles, from an original 11.1 Ah (SoH=100%) at point "1" to a poor 0.55 Ah (SoH=5%) at point "2". The relatively high capacity fade rate was obtained by means of the accelerated oxidation from atmospheric oxygen (after exclusion of the nitrogen purge) combined with the small system size. By the end of the 50th cycle, there was a significant volume change in favour of the negolyte ($V_n = 320$ ml, $V_p = 260$ ml), which is consistent with the used anionic membrane [10].

At that point, the two-step optimal remixing procedure presented in the flowchart of figure 4b was carried out to recover the battery capacity. Specifically, this involved the following steps:

1. The total volume of electrolyte was calculated, as the sum of the initial volume in each tank: $V_t = V_p^i + V_n^i = 580$ ml.

2. A total remixing was carried out, as described in section 3.3.

3. Two complete cycles were performed, during which the VFB capac-

ity was measured as described in section 3.2. It was found that the total remixing resulted in a partial capacity recovery up to 4.1 Ah (SoH=37%) at point "3" of figure 5a, which slightly decreased to 3.8 Ah (SoH=34%) in the following cycle.

4. The SoH was calculated by comparing the total capacity with the initial one, when the system was perfectly balanced: $\mathrm{SoH^i} = \frac{3.8\ \mathrm{Ah}}{11.1\ \mathrm{Ah}} = 0.34$.

5. Since the total remixing had just been performed, volumes and concentrations were equalised, and thus it was assumed that $\Delta m \approx 0$. Therefore, it was inferred that the capacity loss at this point was exclusively originated by faradaic imbalance, i.e., by oxidation. From (8) it was obtained that $\Delta q^i = 1 - \mathrm{SoH^i} = 1 - 0.34 = 0.66$.

6. The target stoichiometric imbalance was calculated as $\Delta m^f = (2/3) \times 0.66 = 0.44$.

7. Since volumes and concentrations were equalised in the total remixing, it was assumed that the number of vanadium moles at the negative side ($M_n^i = M_2^i + M_3^i$) was the same as the number of moles at the positive side ($M_p^i = M_4^i + M_5^i$), and the total concentrations were equal to the initial concentration c_v. Applying the definition of Δm given in (5), and considering that the number of moles that are tansferred in the optimal remixing operation are equal to $c_v \Delta V$, it was obtained that

$$\Delta m^f = \frac{M_p^f - M_n^f}{M_t/2} = \frac{(M_p^i + c_v \Delta V) - (M_n^i + c_v \Delta V)}{c_v V_t/2} = 4\frac{\Delta V}{V_t},$$

which yielded that the volume to be transferred was

$$\Delta V = \Delta m^f \frac{V_t}{4} = 0.44 \frac{580\mathrm{ml}}{4} = 63.8\mathrm{ml}$$

8. The optimal remixing was conducted by transferring 64 ml from the negative tank to the positive one, using a pipette.

The optimal remixing resulted in a dramatic recovery of the battery capacity at a value of 8.2 Ah (SoH = 78%, point "4"). Remarkably, this result represented a recovery of a 66% of the capacity loss in comparison with the condition of perfectly balanced electrolyte masses ($\Delta m = 0$), which matched very accurately the theoretical prediction of two-thirds (66.6%).

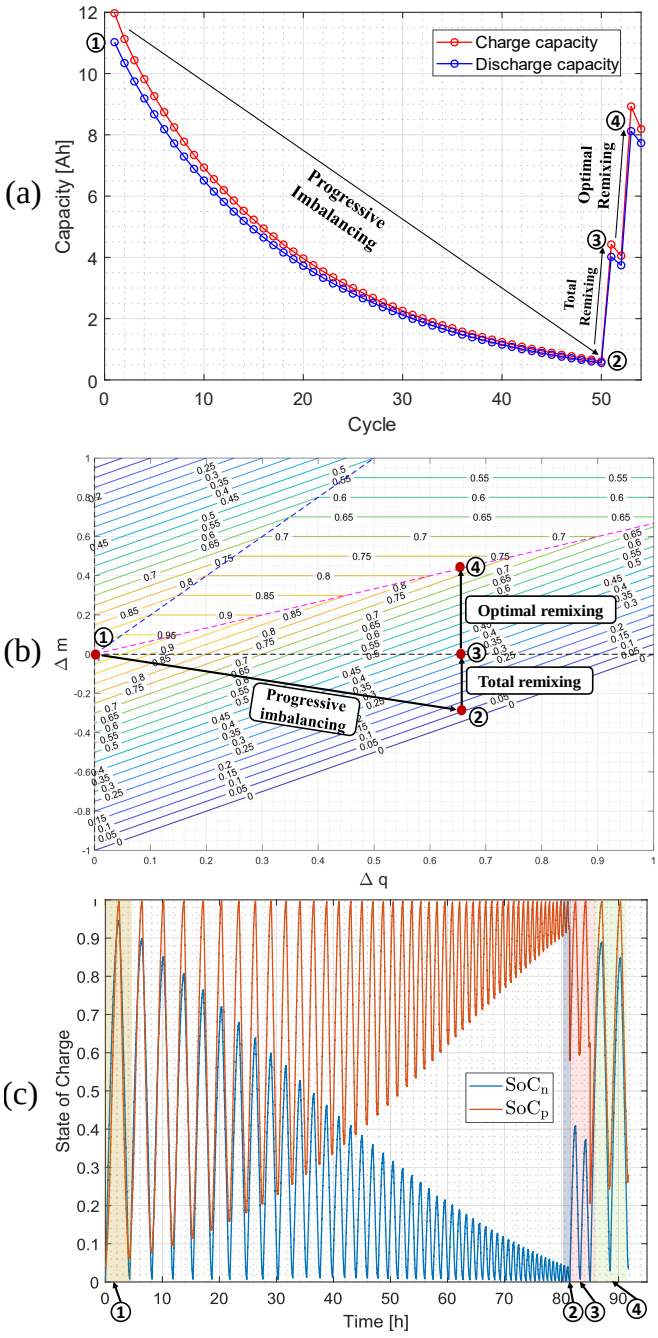

Figure 5: a) Capacity evolution as the battery becomes progressively imbalanced and subsequent recovery attained by total and optimal remixing. The bypass valve is closed throughout Test 1. b) Trajectory of the process in the $\Delta q - \Delta m$ imbalance map. c) States of Charge of the negolyte and posolyte during the first part of Test 1.

Figure 5b displays the trajectory of the process in a zoomed part of the imbalance map of Figure 2b. It can be appreciated than both oxidation and crossover towards the negative half-cell contributed to the capacity loss occurring from points "1" to "2". The limited effectiveness of the total remixing in recovering the capacity (point "3") is ascribable to the major contribution of oxidation to imbalance. The figure also shows why a positive stoichiometric imbalance ($\Delta m > 0$, with more electrolyte in the positive tank), allowed to maximise the capacity. Indeed, the optimal remixing consisted in inducing such positive imbalance and reach the capacity isoline of 78% at point "4".

The evolution of the two SoCs during the process is shown in Figure 5c. As the VFB becomes imbalanced, the posolyte SoC becomes higher than the negolyte SoC, so that in charge a part of V^{III} ions at the negolyte cannot be reduced to V^{II} because of the lack of the V^{IV} counterpart at the posolyte when SoC_p approaches 1. Similarly, in discharge a part of V^{V} cannot be transformed into V^{IV}, which results in narrowing the available SoCs range. When the remixing operations are conducted, this window is significantly expanded, hence attaining a recovery of the battery capacity, especially in the case of optimal remixing.

To further prove the soundness of the imbalance map of Figure 2b, an excessive electrolyte transfer towards the posolyte ($V_p = 370$ ml and $V_n = 210$ ml) was applied after the first 54 cycles, leading the system to a condition above the optimal capacity line ($\Delta m = 2/3\Delta q$) that separates zones A.1 from A.2. Then, 12 additional cycles were performed, whose capacity evolution and trajectory in the imbalance map are displayed in Figures 6a and 6b, respectively. Since the the system was initially in zone A.2 of Figure 2b, the progression of oxidation was expected to have no effect on the VFB capacity, while the crossover towards the negative half-cell that spontaneously occurred in the anionic membrane was expected to have a beneficial effect on the capacity. This behaviour was confirmed during the first 7 cycles of Figure 6a, where a gradual capacity increase was observed. Once the system crossed the optimal capacity line from zone A.2 to zone A.1, both oxidation and crossover started to negatively affect the battery SoH, hence initiating a sharp capacity decay.

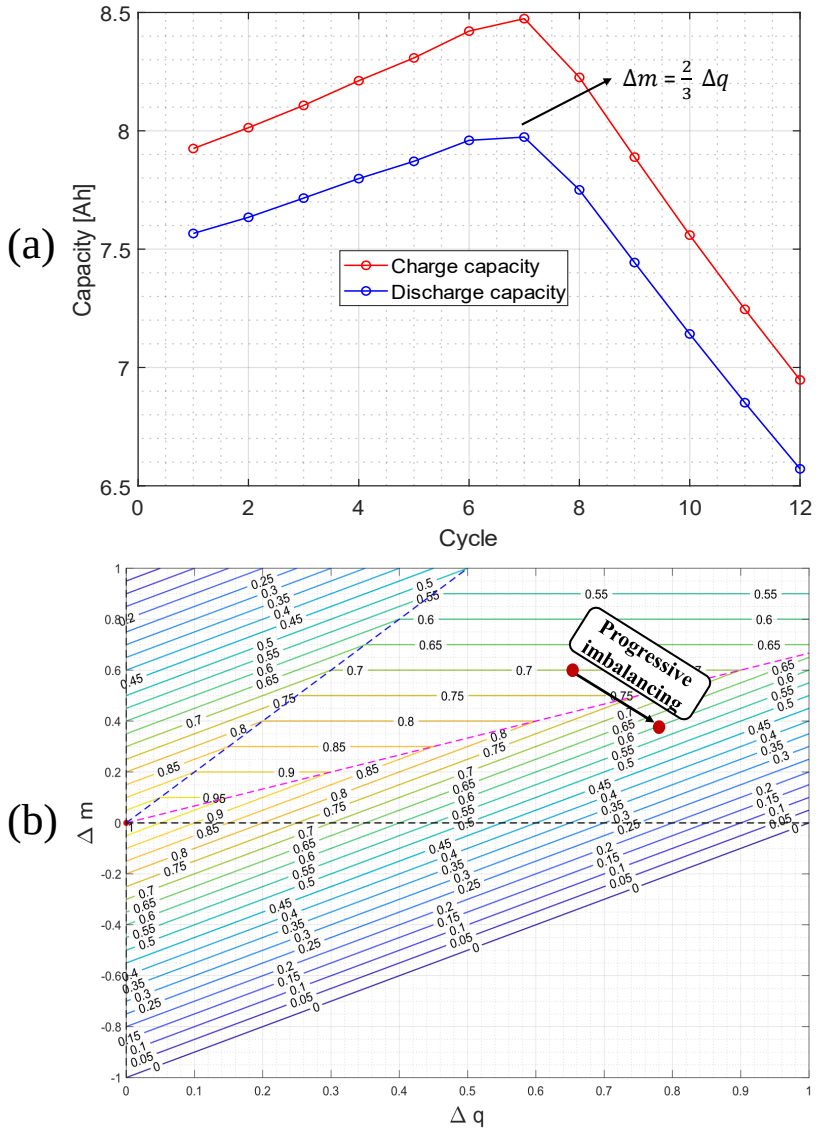

Figure 6: a) Capacity evolution when the VFB starts from a condition above the optimal capacity line. b) Trajectory of the system on the $\Delta q - \Delta m$ imbalance map.

4.2. Test 2: effect of the bypass pipe

The second test was intended to assess the effectiveness of the bypass pipe in mitigating the battery capacity loss. The test pattern was similar to Test 1: starting from a balanced condition the battery underwent 50 cycles; then,

a total remixing was performed and two additional cycles were run; finally, an optimal remixing was conducted which was followed by two final cycles. The bypass valve was kept open throughout the whole test, except in the last two cycles when a closed valve allowed keeping the desired stoichiometric imbalance.

The resulting capacity profile is displayed in Figure 7a. Although the bypass pipe has a beneficial effect in slowing down the capacity decay, the effectiveness of this method is very limited. After 50 cycles, the capacity had decreased from 11.2 Ah at point "1" to 1.3 Ah at point "2". The explanation to this behaviour is that the bypass pipe is only able to minimise the stoichiometric imbalance, by counteracting possible volumetric changes, thus keeping the value of Δm close to 0, but it is not able to compensate the oxidation that constitutes the main source of imbalance in this system. Note that, as a result of possible concentration imbalances, Δm may present small deviations from 0, as appreciated at point "2" of the trajectory shown in figure 7b. After performing the total remixing, the capacity decreased even more instead of recovering, possibly due to a residual concentration imbalance not compensated by the bypass pipe. Consequently, if this imbalance was towards the positive half cell, its correction was actually counterproductive for the battery capacity (points "2" and "3" of Figure 7b).

Finally, the optimal remixing operation was run, following the same steps as in Test 1. This resulted in a transfer of 96 ml from the negative electrolyte to the positive one, which allowed to achieve a capacity of 7.3 Ah (SoH = 65%) at point "4". This was a highly satisfactory result, given that with stoichiometrically balanced electrolytes (i.e. same volumes and concentrations, as in point "3"), the capacity was already reaching a value close to 0. In other words, with a traditional approach, the battery capacity would be completely exhausted unless a chemical/electrochemical regeneration was conducted.

Figure 7c compares the time evolution of the capacity during the first 50 cycles of tests 1 and 2, showing that the bypass pipe had a beneficial effect. Although in both cases the capacity eventually reached very low values, the rate of decrease was considerably slower in the second case, as a result of the compensation of the contribution of stoichiometric imbalance to the capacity loss. Naturally, this beneficial effect would be much more significant in a system with slow oxidation, where crossover is the main cause of imbalance. Additionally, this figure allows to see that the capacity loss process was almost linear in time, i.e., that the concavity of the capacity evolution plots

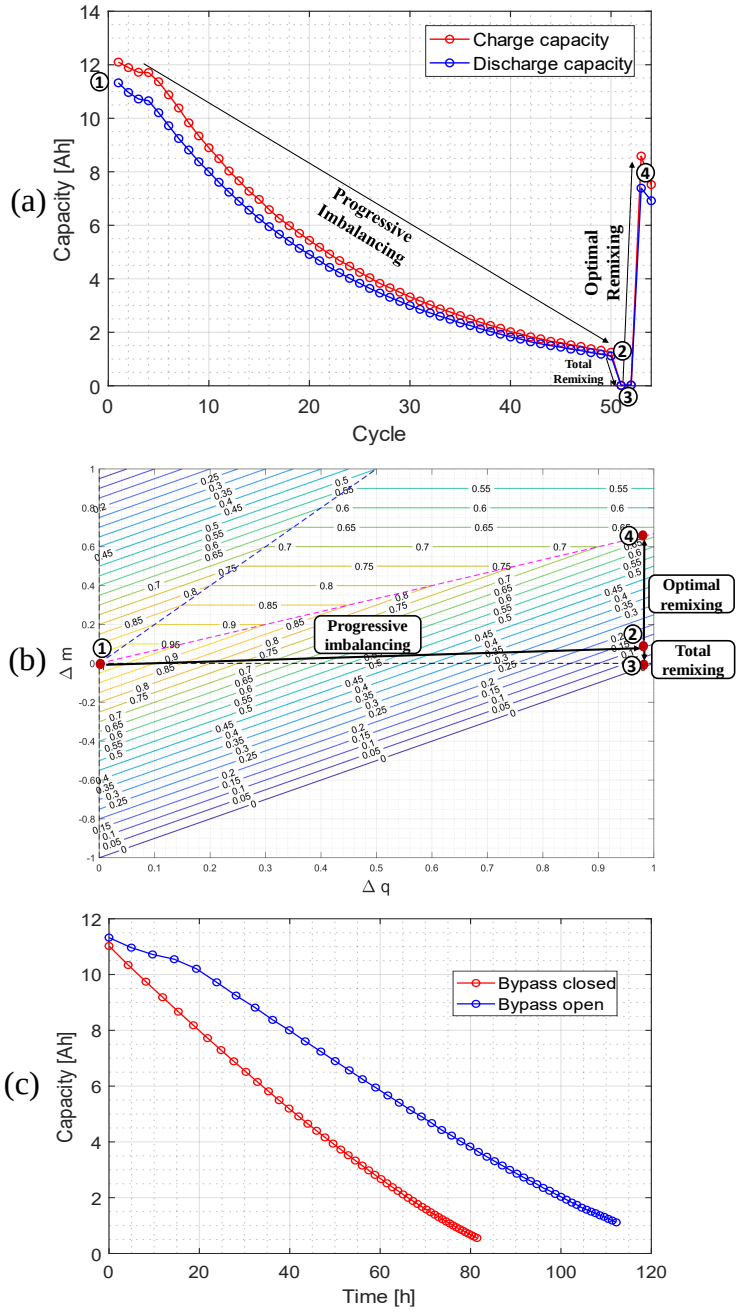

Figure 7: a) Capacity evolution as the battery became progressively imbalanced and subsequent recovery attained by total and optimal remixing. The bypass valve was open throughout the whole Test 2, except in the last two cycles. b) Trajectory of the system on the $\Delta q - \Delta m$ imbalance map. c) Comparison of the capacity evolution in the first 50 cycles of Test 1 (bypass closed) and Test 2 (bypass open).

of Figs. 5a and 7a was not originated by a reduction of the oxidation rate, but by a gradual decrease in the cycle duration. Interestingly, since the average concentration of V^{2+} decreased as the imbalance progressed (see Figure 5c), this result implies that the oxidation reaction rate was almost zero order with respect to V^{2+} concentration. In turn, it emerges that the mass transfer of oxygen from the exterior of the tank to the surface of the electrolyte was the limiting factor of the reaction rate.

4.3. Test 3: periodical rebalancing operations

The third test aimed to demonstrate the proposal when frequent rebalancing operations were performed. Specifically, the total and the optimal remixing were conducted every 10 cycles over a total of 50 cycles, in order to cover a wider range of oxidation levels, as well as to provide clues on the practical implementation of the proposed method. Although this frequency is considerably higher than that expected in a real application, it results useful to illustrate the operativeness the method, given the fast oxidation rate observed in the system under study. The bypass valve was kept closed throughout the whole test, in order to preserve the mass imbalances induced with the optimal remixing operations.

The capacity evolution during this test is presented in Figure 8. Starting from a value of 11.2 Ah, it decreased to 5.2 Ah (SoH = 46%) after the first 10 cycles. Following the total remixing, a modest recovery was observed, reaching a capacity of 6.8 Ah (SoH = 61%). In turn, upon performing the optimal remixing, a remarkable recovery was achieved up to 10.1 Ah (SoH = 90%). After the next 10 cycles, another total remixing was performed, which had a counterproductive effect of reducing the capacity from 4 Ah to 0.6 Ah. This adverse effect was due to the fact that, since an optimised remixing had been previously conducted, the system already had a positive value of Δm at cycle 21 ($V_n = 260$ ml and $V_p = 320$ ml), with a beneficial effect in Zone A.1 of the map 2b. Then, when the total remixing was run, Δm was set to 0 and the VFB moved even further away from the optimal capacity line. When the second optimal remixing was carried out, a substantial capacity recovery at 8.9 Ah (79%) was attained.

In the remaining cycles, the oxidation level was so high that the capacity collapsed to zero when the total remixing was performed, meaning that Δq was equal or greater than 1, i.e., an AOS ≥ 4. Therefore, since any value of $\Delta q \geq 1$ could correspond to this condition, it was not possible to quantify the exact value of the faradaic imbalance by just measuring the resulting capacity

after the total remixing. When the third partial remixing was performed assuming a value of $\Delta q = 1$, only a limited recovery took place, indicating that the actual value of Δq was probably higher than 1. To confront this situation, the last two optimal remixing operations were performed without previously conducting the total remixing. Instead, the initial value of Δm was estimated from the volume difference between the two tanks assuming that the two concentrations are equal, as: $\Delta m = 2(V_p - V_n)/(V_p + V_n)$. Then, the value of Δq that allows to calculate target Δm^f was obtained directly by solving (8). Although these last cycles corresponded to extreme values of oxidation hardly occurring in a real system, they were useful to demonstrate how the developed strategy allows to keep in service a VFB that would be otherwise completely exhausted. For instance, at cycle 44 of Figure 8, a capacity of 5.7 Ah (SoH = 51%) was attained for an AOS ≈ 4.24.

As a final remark, it should be emphasised that, in this research the optimal remixing was normally conducted after a total remixing, assuming that concentration measurements were not available. However in real applications where such information is available (thus also Δm and Δq are), such intermediate step is not necessary. In that case, the one-step variant of the optimal remixing presented in Figure 4a can be applied.

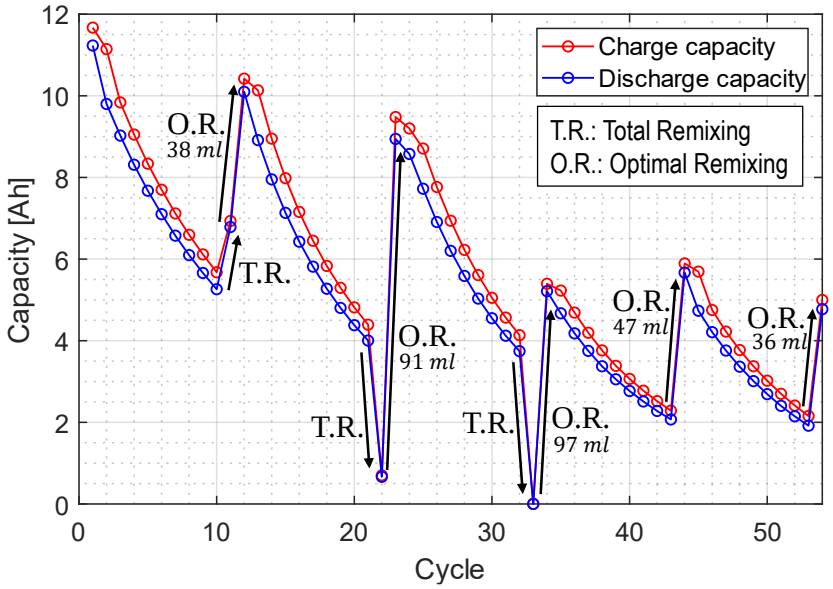

Figure 8: Capacity evolution with frequent rebalancing operations, indicating the volume of solution transferred from the negative tank to the positive tank in each O.R. operation.

5. Conclusion

The performance of different methods for minimising the capacity loss in vanadium flow batteries suffering from electrolyte imbalance has been experimentally investigated. Specifically, a novel optimal remixing procedure was implemented and compared to the conventional total remixing and the bypass connection between tanks. Special attention was given to the combined effect of stoichiometric imbalance, originated from membrane crossover, and faradaic imbalance, originated from oxidative or reductive side reactions that produce a shift in the average oxidation state of the electrolyte.

It has been shown that the effectiveness of the total remixing and the hydraulic bypass is very limited when oxidation constitutes the primary cause of imbalance. Furthermore, it was demonstrated that under certain imbalance conditions the total remixing can actually have a counterproductive effect, leading to a lower capacity instead of a recovery. In contrast, the capacity loss associated to oxidative imbalance can be substantially mitigated by applying the optimal mass imbalance, namely, by transferring a calculated volume of electrolyte from the negative to the positive electrolyte based on the deviation of the AOS from the ideal value of +3.5. We have obtained solid experimental results, highly consistent with the theoretical predictions, demonstrating that the final capacity loss achieved with the optimal mass imbalance is only a 33% of the final capacity loss after total remixing, i.e., with perfectly balanced electrolyte masses. Therefore, the proposed method allows to keep in operation a vanadium flow batteries with an acceptably high capacity, which would otherwise suffer from an unacceptable level of capacity loss.

The encouraging results obtained in this work show that the optimal remixing constitutes a simple and cost-effective method to substantially mitigate the effects of electrolyte imbalance, making it particularly appealing for those facilities that lack of a chemical/electrochemical regeneration system. To the best of our knowledge, the proposed method is the only experimentally validated one that considers the impact of both types of imbalance on the battery capacity, as well as the only one that allows to recover capacity loss associated with faradaic imbalance without resorting to any additional equipment or reactant. Moreover, it is highlighted that the optimal remixing is of simple implementation and can be applied to any VFB system, regardless of its size, electrodes and membrane materials, active species concentrations, and operating conditions. Finally, the proposed method can also

be extended to other flow battery chemistries provided that they are based on a single active element.

Acknowledgements

The project that gave rise to these results received the support of a fellowship from "la Caixa" Foundation (ID 100010434). The fellowship code is LCF/BQ/DI21/11860023. This research was also supported by the Spanish Ministry of Science and Innovation, under the projects MAFALDA (PID2021-126001OB-C31) and MASHED (TED2021-129927B-I00). This work has been supported by the Spanish Ministry of Universities funded by the European Union - NextGenerationEU (2022UPC-MSC-93823). On the Italian side, funding were granted by "NEST – Network 4 Energy Systainable Transition" (MUR PE000021) within the Piano Nazionale di Ripresa e Resilienza (PNRR).

References

[1] European Commission Directorate-General for Energy, Renewable energy – directive, targets and rules (2023). Available online: https://energy.ec.europa.eu/topics/renewable-energy/renewable-energy-directive-targets-and-rules_en.

[2] M. Y. Suberu, M. W. Mustafa, N. Bashir, Energy storage systems for renewable energy power sector integration and mitigation of intermittency, Renewable and Sustainable Energy Reviews 35 (2014) 499–514. doi:10.1016/j.rser.2014.04.009.

[3] C. Breyer, S. Khalili, D. Bogdanov, M. Ram, On the history and future of 100 % renewable energy systems research, IEEE Access 10 (2022) 78176–78218. doi:10.1109/ACCESS.2022.3193402.

[4] A. A. Kebede, T. Kalogiannis, J. V. Mierlo, M. Berecibar, A comprehensive review of stationary energy storage devices for large scale renewable energy sources grid integration, Renewable and Sustainable Energy Reviews 159 (5 2022). doi:10.1016/j.rser.2022.112213.

[5] M. Guarnieri, A. Trovò, A. D'Anzi, P. Alotto, Developing vanadium redox flow technology on a 9-kw 26-kwh industrial scale test facility:

Design review and early experiments, Applied Energy 230 (2018) 1425–1434. doi:10.1016/j.apenergy.2018.09.021.

[6] Z. Zhang, T. Ding, Q. Zhou, Y. Sun, M. Qu, Z. Zeng, Y. Ju, L. Li, K. Wang, F. Chi, A review of technologies and applications on versatile energy storage systems, Renewable and Sustainable Energy Reviews 148 (9 2021). doi:10.1016/j.rser.2021.111263.

[7] Z. Huang, A. Mu, Research and analysis of performance improvement of vanadium redox flow battery in microgrid: A technology review, International Journal of Energy Research 45 (2021) 14170–14193. doi:10.1002/er.6716.

[8] T. Jirabovornwisut, A. Arpornwichanop, A review on the electrolyte imbalance in vanadium redox flow batteries, International Journal of Hydrogen Energy 44 (2019) 24485–24509. doi:10.1016/j.ijhydene.2019.07.106.

[9] Z. Yang, R. M. Darling, M. L. Perry, Electrolyte compositions in a vanadium redox flow battery measured with a reference cell, Journal of The Electrochemical Society 166 (2019) A3045–A3050. doi:10.1149/2.1161913jes.

[10] T. Puleston, A. Clemente, R. Costa-Castelló, M. Serra, Modelling and estimation of vanadium redox flow batteries: A review, Batteries 8 (9 2022). doi:10.3390/batteries8090121.

[11] M. Nourani, C. R. Dennison, X. Jin, F. Liu, E. Agar, Elucidating effects of faradaic imbalance on vanadium redox flow battery performance: Experimental characterization, Journal of The Electrochemical Society 166 (2019) A3844–A3851. doi:10.1149/2.0851915jes.

[12] P. Loktionov, A. Pustovalova, R. Pichugov, D. Konev, A. Antipov, Quantifying effect of faradaic imbalance and crossover on capacity fade of vanadium redox flow battery, Electrochimica Acta (2024) 144047doi:doi.org/10.1016/j.electacta.2024.144047.

[13] O. Nolte, I. A. Volodin, C. Stolze, M. D. Hager, U. S. Schubert, Trust is good, control is better: A review on monitoring and characterization techniques for flow battery electrolytes, Materials Horizons 8 (2021) 1866–1925. doi:10.1039/d0mh01632b.

[14] N. Poli, M. Schäffer, A. Trovò, J. Noack, M. Guarnieri, P. Fischer, Novel electrolyte rebalancing method for vanadium redox flow batteries, Chemical Engineering Journal 405 (2 2021). doi:10.1016/j.cej.2020.126583.

[15] Y. Zhang, L. Liu, J. Xi, Z. Wu, X. Qiu, The benefits and limitations of electrolyte mixing in vanadium flow batteries, Applied Energy 204 (2017) 373–381. doi:10.1016/j.apenergy.2017.07.049.

[16] S. Corcuera, M. Skyllas-Kazacos, State-of-charge monitoring and electrolyte rebalancing methods for the vanadium redox flow battery, European Chemical Bulletin 1 (2012) 511–519.

[17] K. E. Rodby, T. J. Carney, Y. A. Gandomi, J. L. Barton, R. M. Darling, F. R. Brushett, Assessing the levelized cost of vanadium redox flow batteries with capacity fade and rebalancing, Journal of Power Sources 460 (6 2020). doi:10.1016/j.jpowsour.2020.227958.

[18] M. Skyllas-Kazacos, C. Menictas, The vanadium redox battery for emergency back-up applications, in: Proceedings of Power and Energy Systems in Converging Markets, 1997, pp. 463–471. doi:10.1109/INTLEC.1997.645928.

[19] A. Bhattarai, N. Wai, R. Schweiss, A. Whitehead, G. G. Scherer, P. C. Ghimire, T. M. Lim, H. H. Hng, Vanadium redox flow battery with slotted porous electrodes and automatic rebalancing demonstrated on a 1 kw system level, Applied Energy 236 (2019) 437–443. doi:10.1016/j.apenergy.2018.12.001.

[20] M. Y. Lu, W. W. Yang, Y. M. Deng, W. Z. Li, Q. Xu, Y. L. He, Mitigating capacity decay and improving charge-discharge performance of a vanadium redox flow battery with asymmetric operating conditions, Electrochimica Acta 309 (2019) 283–299. doi:10.1016/j.electacta.2019.04.032.

[21] J. Shin, C. Kim, B. Jeong, N. Vaz, H. Ju, New operating strategy for all-vanadium redox flow batteries to mitigate electrolyte imbalance, Journal of Power Sources 526 (4 2022). doi:10.1016/j.jpowsour.2022.231144.

[22] F. Toja, L. Perlini, D. Facchi, A. Casalegno, M. Zago, Dramatic mitigation of capacity decay and volume variation in vanadium redox flow

batteries through modified preparation of electrolytes, Applied Energy 354 (2024) 122262. doi:https://doi.org/10.1016/j.apenergy.2023.122262.

[23] L. Cao, M. Skyllas-Kazacos, C. Menictas, J. Noack, A review of electrolyte additives and impurities in vanadium redox flow batteries, Journal of Energy Chemistry 27 (2018) 1269–1291. doi:10.1016/j.jechem.2018.04.007.

[24] D. Cremoncini, G. F. Frate, A. Bischi, L. Ferrari, Mixed integer linear program model for optimized scheduling of a vanadium redox flow battery with variable efficiencies, capacity fade, and electrolyte maintenance, Journal of Energy Storage 59 (2023) 106500. doi:doi.org/10.1016/j.est.2022.106500.

[25] S. C. Chieng, M. Kazacos, M. Skyllas-Kazacos, Preparation and evaluation of composite membrane for vanadium redox battery applications, Journal of Power Sources 39 (1992) 11–19. doi:10.1016/0378-7753(92)85002-R.

[26] N. Roznyatovskaya, T. Herr, M. Küttinger, M. Fühl, J. Noack, K. Pinkwart, J. Tübke, Detection of capacity imbalance in vanadium electrolyte and its electrochemical regeneration for all-vanadium redox-flow batteries, Journal of Power Sources 302 (2016) 79–83. doi:10.1016/j.jpowsour.2015.10.021.

[27] Z. Li, L. Liu, Y. Zhao, J. Xi, Z. Wu, X. Qiu, The indefinite cycle life via a method of mixing and online electrolysis for vanadium redox flow batteries, Journal of Power Sources 438 (10 2019). doi:10.1016/j.jpowsour.2019.226990.

[28] R. Pichugov, P. Loktionov, A. Pustovalova, A. Glazkov, A. Grishko, D. Konev, M. Petrov, A. Usenko, A. Antipov, Restoring capacity and efficiency of vanadium redox flow battery via controlled adjustment of electrolyte composition by electrolysis cell, Journal of Power Sources 569 (6 2023). doi:10.1016/j.jpowsour.2023.233013.

[29] M. Skyllas-Kazacos, B. Maddern, M. Kazacos, State of charge of redox cell, World Intelectual Property Organization, Patent PCT/AU89/00252 (1989).

[30] G. Kazacos, N. Kazacos, Improved perfluorinated membranes and improved electrolytes for redox cells and batteries, World Intelectual Property Organization, Patent PCT/AU89/00252 (2006).

[31] N. Poli, A. Trovò, P. Fischer, J. Noack, M. Guarnieri, Electrochemical rebalancing process for vanadium flow batteries: Sizing and economic assessment, Journal of Energy Storage 58 (2 2023). doi:10.1016/j.est.2022.106404.

[32] T. Puleston, M. Serra, R. Costa-Castelló, Vanadium redox flow battery capacity loss mitigation strategy based on a comprehensive analysis of electrolyte imbalance effects, Applied Energy 355 (2024) 122271. doi:10.1016/j.apenergy.2023.122271.

[33] A. Trovò, M. Guarnieri, Battery management system with testing protocols for kw-class vanadium redox flow batteries, in: 2020 2nd IEEE International Conference on Industrial Electronics for Sustainable Energy Systems (IESES), Vol. 1, 2020, pp. 33–38. doi:10.1109/IESES45645.2020.9210697.

[34] Y. Li, L. Sun, L. Cao, J. Bao, M. Skyllas-Kazacos, Dynamic model based membrane permeability estimation for online soc imbalances monitoring of vanadium redox flow batteries, Journal of Energy Storage 39 (7 2021). doi:10.1016/j.est.2021.102688.

[35] S. Ressel, F. Bill, L. Holtz, N. Janshen, A. Chica, T. Flower, C. Weidlich, T. Struckmann, State of charge monitoring of vanadium redox flow batteries using half cell potentials and electrolyte density, Journal of Power Sources 378 (2018) 776–783. doi:10.1016/j.jpowsour.2018.01.006.

[36] J. Geiser, H. Natter, R. Hempelmann, B. Morgenstern, K. Hegetschweiler, Photometrical determination of the state-of-charge in vanadium redox flow batteries part i: In combination with potentiometric titration, Zeitschrift für Physikalische Chemie 233 (12) (2019) 1683–1694. doi:10.1515/zpch-2019-1379.

[37] C. Stolze, P. Rohland, K. Zub, O. Nolte, M. D. Hager, U. S. Schubert, A low-cost amperometric sensor for the combined state-of-charge, capacity, and state-of-health monitoring of redox flow battery electrolytes, Energy Conversion and Management: X 14 (2022) 100188. doi:https://doi.org/10.1016/j.ecmx.2022.100188.

[38] T. Puleston, A. Cecilia, R. Costa-Castelló, M. Serra, Nonlinear observer for online concentration estimation in vanadium flow batteries based on half-cell voltage measurements, Computers and Chemical Engineering 185 (2024) 108664. doi:https://doi.org/10.1016/j.compchemeng.2024.108664.

[39] P. Jienkulsawad, T. Jirabovornwisut, Y. S. Chen, A. Arpornwichanop, Improving the performance of an all-vanadium redox flow battery under imbalance conditions: Online dynamic optimization approach, ACS Sustainable Chemistry and Engineering 8 (2020) 13610–13622. doi:10.1021/acssuschemeng.0c02973.